Graph Polynomial Convolution Models for Node Classification of Non-Homophilous Graphs

Kishan Wimalawarne[1] and Taiji Suzuki[1,2]

[1]Department of Mathematical Informatics, The University of Tokyo, Tokyo, Japan
[2]Center for Advanced Intelligence Project (AIP), RIKEN, Tokyo, Japan

Abstract

We investigate efficient learning from higher-order graph convolution and learning directly from adjacency matrices for node classification. We revisit the scaled graph residual network and remove ReLU activation from residual layers and apply a single weight matrix at each residual layer. We show that the resulting model lead to new graph convolution models as a polynomial of the normalized adjacency matrix, the residual weight matrix, and the residual scaling parameter. Additionally, we propose adaptive learning between directly graph polynomial convolution models and learning directly from the adjacency matrix. Furthermore, we propose fully adaptive models to learn scaling parameters at each residual layer. We show that generalization bounds of proposed methods are bounded as a polynomial of eigenvalue spectrum, scaling parameters, and upper bounds of residual weights. By theoretical analysis, we argue that the proposed models can obtain improved generalization bounds by limiting the higher-orders of convolutions and direct learning from the adjacency matrix. Using a wide set of real-data, we demonstrate that the proposed methods obtain improved accuracy for node-classification of non-homophilous graphs.

1 Introduction

Graph convolution networks have become a highly active research area among the machine learning and deep learning researchers in recent years. Their success in many widely growing application areas such as social influence prediction Li and Goldwasser (2019), relationship modelling Schlichtkrull et al. (2018), recommendation systems Ying et al. (2018), and computer vision Zhao et al. (2019), have made both the academia and the industry indentify the significance graph convolution networks. Despite the many graph convolution networks available, the optimal use of convolution of features and graph structure for efficient learning is still widely open for research from perspectives of both model design and theoretical understanding.

One of the challenging problem in graph convolution networks is learning from graphs with various homophily conditions McPherson et al. (2001). Homophily of a graph dictates the way labeled nodes link with other labeled nodes. When nodes have the tendency to link with other nodes with the same label such graphs are known to be homophilous, while graphs with nodes that have more tendency to link with nodes with different labels are known as non-homophilous McPherson et al. (2001); Chien et al. (2021). In early research, most graph convolution networks have been developed by evaluating node classification accuracy against the popular benchmark highly homophilous graph datasets such as Cora, Citeseer, and Pubmed Kipf and Welling (2017); Wu et al. (2019). Recently, learning from non-homophilous graphs has gained considerable attention and new homophily measures and non-homophilous graph datasets have been introduced Zhu et al. (2020); Lim et al. (2021b) imposing new challenges to existing graph convolution networks.

Graph convolution networks that have been developed for non-homophilous graphs are limited. One of the strategy employed in learning from non-homophilous graphs is feature learning by using convolutions from higher-order neighbors of nodes. MixHop Abu-El-Haija et al. (2019) and GPRGNN Chien et al. (2021) employed this approach by using higher-orders of the normalized adjacency matrix with concatenations and the generalised Pagerank, respectively. However, recent studies Zhu et al. (2020); Lim et al.

(2021b) using noval non-homophilous graph datasets have shown that only learning from node features or the adjacency matrix can provide competitive accuracy for node classification against popular GCN models. As we show in the Table 1, learning solely on the adjacency matrix using the LINK Zheleva and Getoor (2009) for Squirrel and learning only using the node features by a MLP for Film have obtained the best node classification accuracy compared to more sophisticated graph convolution models such as GCN or GPRGNN. The recently developed LINKX Lim et al. (2021b) is another simple model using MLPs on node features and the adjacency matrix separately prior to concatenation. Though LINKX has no explicit graph convolution it has recorded competitive node classification accuracies Lim et al. (2021b) for non-homophilous graphs outperforming many state of the art graph convolution networks. These recent developments have made us re-think on the efficient use of node features and graph strcuture for node classification.

Dataset	Squirrel	Film
MLP	30.10±2.00	**37.38±0.85**
LINK	**62.69±1.69**	25.24±1.12
GCN	46.23±2.26	27.61±0.95
GPRGNN	51.19±1.41	35.46±0.92
LINKX	61.81±1.80	36.10±1.55

Table 1: Learning only from node features (MLP) or the adjacency matrix (LINK) compared to convolution models

In this paper, we investigate learning models that adaptively learn by applying adequate graph convolution and direct learning from graph data for a given node classfication problem. In order to improve the graph convolution, we first revisit the scaled residual graph convolution model and apply simplifying graph convolution by removing ReLU activation from residual layers. We show that the resulting model is a graph polynomial convolution model with higher-orders of the adjacency matrices similar to the generalized Pagerank. However, our model also has higher-orders of weights making it a polynomial of both adjacency matrices and weights allowing nonlinear feature mixing. We further propose a hybrid model to combine the graph polynomial convolution and direct learning from the adjacency matrix using adaptive scaling. Furthermore, we propose fully adaptive learning models that learn coefficients of residual layers as well as the scaling parameters between graph convolution and direct learning from the adjacency matrix. We analyse generalization bounds of the proposed models using transductive Rademacher complexity and show that our models have better generalization due to polynomial structure of graph convolution and direct learning from adjacency matrices. We evaluate our proposed models on node classification using several benchmark real-data sets and show that our proposed models give improved performances or comparable performances for non-homophilous graphs compared to existing state of the art methods.

2 Review

This section contains a brief overview of graph homophily and graph convolution networks to provide motivations for our research.

We start with stating the notations used in this paper. A graph is represented by $G = (V, E)$ with nodes by $v_i \in V$, $i = 1, \ldots, N$ and edges by $(v_i, v_j) \in E$. Let $X \in \mathbb{R}^{N \times q}$ represents a feature matrix with q features. Let $Y \in \mathbb{R}^{N \times C}$ represents C-labels of the N nodes. We consider node classification problem where each node $v \in V$ belongs to a class $y_v \in \{0, 1, \ldots, C - 1\}$. The adjacency matrix of G is represented as $A \in \mathbb{R}^{N \times N}$, and the self-loops added adjacency matrix is $\hat{A} = A + I_N$, where $I_N \in \mathbb{R}^{N \times N}$ is a identity matrix. We denote the diagonal degree matrix of $\hat{A}$ by $\hat{D}_{ij} = \sum_k \hat{A}_{ik} \delta_{ij}$, then the normalized adjacency matrix is $\tilde{A} = \hat{D}^{-1/2} \hat{A} \hat{D}^{-1/2}$.

2.1 Graph Homophily

An important property of a graph is the way labeled nodes form links with adjacent nodes, which is known as the homophily of a graph. The homophily ratio McPherson et al. (2001); Chien et al. (2021) (a.k.a edge homophily Lim et al. (2021a)) is the fraction of edges in a graph that connect nodes with the same class label defined as

$$\mathcal{H}(G) = \frac{|\{(u, v) : (u, v) \in E \wedge y_u = y_v\}|}{|E|}.$$

Based on the edge homophily ratio, a graph is called homophilous when $\mathcal{H}(G) \to 1$ and non-homophilous when $\mathcal{H}(G) \to 0$.

Recently, Lim et al. (2021b,a) have shown that under class-imbalance conditions, when the majority of the nodes belong to a single class label, then these graphs have edge homophily ratio close to 1. To properly reflect homophily under the

class-imbalance condition, a new homophily measure Lim et al. (2021b) was proposed as

$$\hat{\mathcal{H}}(G) = \frac{1}{C-1} \sum_{k=0}^{C-1} \left[h_k - \frac{|C|}{n} \right]_+,$$

where $[a]_+ = \max\{a, 0\}$, C is the number of classes, and h_k is the class-wise homophily matrix defined by

$$h_k = \frac{\sum_{x \in C_x} d_x^{(k_x)}}{\sum_{x \in C_x} d_x},$$

where d_x is the number of neighbours, $k_x \in \{0, 1, \ldots, C-1\}$ is the class label of the node x, and $d_x^{(k_x)}$ is the number of neighbors with same label as the node x. Similar to the edge homophily, $\hat{\mathcal{H}}(G) \in [0, 1]$, and a graph is recognised as non-homophilous when $\hat{\mathcal{H}}(G) \to 0$.

2.2 Graph Convolutional Models

The most basic model to apply graph convolution is the initial model proposed by Kipf and Welling (2017), which is often referred to as the Vanilla GCN model. This model multiplies node features $X \in \mathrm{R}^{N \times q}$ by the normalized adjacency matrix $\tilde{A} \in \mathrm{R}^{N \times N}$ and apply ReLU activation at each layer. A 2-layer model is

$$Y = \mathrm{softmax}\big(\tilde{A}\mathrm{ReLU}(\tilde{A}XW_0)W_1\big), \tag{1}$$

where $W_0 \in \mathbb{R}^{q \times h}$ and $W_1 \in \mathbb{R}^{h \times C}$ are learning weights with h hidden units. Wu et al. (2019) proposed the simplifying graph convolution (SGC) model by removing the $\mathrm{ReLU}()$ activation from from the Vanilla GCN model (1) as

$$Y = \mathrm{softmax}\big(\tilde{A}^2 XW_0W_1\big) = \mathrm{softmax}\big(\tilde{A}^2 XW\big),$$

where $W := W_0W_1 \in \mathbb{R}^{q \times C}$. These models have obtained reasonable node classification accuracy for homophilous graphs Chien et al. (2021), however, their accuracy with non-homophilous graphs have high variance Lim et al. (2021a,b); Chien et al. (2021).

One of the method researchers have successfully employed when learning from non-homophilous graphs is convolution of features of a node using features from multiple hops from that node Zhu et al. (2020); Abu-El-Haija et al. (2019). An efficient method to achieve such convolution is by higher-orders of the normalized adjacency matrix as used by GPRGNN Chien et al. (2021). It replaces the normalized adjacency matrix by the Generalized PageRank (GPR) defined as

$$GPR(\gamma) = \sum_{k=0}^{L-1} \gamma_k \tilde{A}^k, \tag{2}$$

where $\gamma \in \mathbb{R}^L$ are GPR coefficients that are either learned or predefined. In GPRGNN, node features are first taken as input to a neural network and then its output is applied with convolution by GPR as

$$Y = \mathrm{softmax}(Z), \ Z = \sum_{k=0}^{L-1} \gamma_k H^{(k)}, \ H^{(k)} = \tilde{A}H^{(k-1)}, \ H_{i:}^{(0)} = f_\theta(X_{i:}). \tag{3}$$

GPRGNN has shown be a versatile methods to learn both from homophilous and non-homophilous graphs.

A recent study on node classification of large-scale non-homophilous graphs Lim et al. (2021a) has revisited LINK Zheleva and Getoor (2009), which only use the adjacency matrix to classify nodes without node features or convolution. Simply, LINK Zheleva and Getoor (2009) learns by only using the adjacency matrix as

$$Y = \mathrm{softmax}(AW),$$

where $W \in \mathbb{R}^{n \times C}$ is a weight matrix. Despite its simplicity, LINK has obtained competitive performances for some non-homophilous graphs compared to well known graph convolution models. LINKX Lim et al. (2021a), an extension of LINK has been proposed by having two multilinear networks to learn from the adjacency matrix and node features separately and combining their outputs with another multilinear network (MLP) as

$$h_A = \mathrm{MLP}(A) \in \mathbb{R}^{n \times h} \ \ h_X = \mathrm{MLP}(X) \in \mathbb{R}^{n \times h}$$
$$Y = \mathrm{MLP}(W\mathrm{concat}(h_A, h_X) + h_A + h_X),$$

where $\mathrm{concat}()$ is concatenation function, and $W \in \mathbb{R}^{n \times 2h}$. Despite its simplicity LINKX has gained considerable accuracy for non-homophilous graphs outperforming many graph convolution models Lim et al. (2021a). However, a limitation of both LINK and LINKX is the lack graph convolution, which could make them deprived of efficient feature learning as used by graph convolution models.

3 Proposed Method

In this section, we investigate methods to learn from graphs by optimally using graph convolution and graph data (adjacency matrix) to overcome limitations of existing methods.

We start by revisiting the residual graph convolution models with L residual layers with scaling by a predefined parameter γ as

$$
\begin{aligned}
X_0 &= \mathrm{ReLU}(XW_0) \\
X_i &= X_{i-1} + \gamma\mathrm{ReLU}(\bar{A}X_{i-1}W_i), \ i = 1, \ldots, L, \\
Y &= \mathrm{softmax}(X_LW_{L+1}),
\end{aligned}
\tag{4}
$$

where $W_0 \in \mathbb{R}^{N \times h}$, $W_i \in \mathbb{R}^{h \times h}$, and $W_{L+1} \in \mathbb{R}^{h \times C}$. We want to remind the reader that applying an appropriate γ to (4) leads to a Euler descritization of a graph ordinary differential equation equivalent to GODE Poli et al. (2019).

3.1 Graph Polynomial Convolution Network

We propose several extensions the general scaled residual network in (4). For the basic setting, we first propose to apply a T-layered multilinear network to the node features X. Next, for each scaled residual layers we propose to use only a single weight $W_1 = W_2 = \cdots = W_L = W_T\mathbb{R}^{h \times h}$. Further, we propose to remove ReLU activation to make (4) to have simplifying graph convolution Wu et al. (2019). The resulting residual graph convolution model is

$$
\begin{aligned}
X_0 &= \mathrm{ReLU}(XW_0) & X_{T+1} &= X_T + \gamma\bar{A}X_TW_T \\
X_1 &= \mathrm{ReLU}(X_0W_1) & X_{T+2} &= X_{T+1} + \gamma\bar{A}X_{T+1}W_T \\
&\ \ \vdots & &\ \ \vdots \\
X_{T-1} &= \mathrm{ReLU}(X_{T-2}W_{T-1}) & X_{T+L} &= X_{T+L-1} + \gamma\bar{A}X_{T+L-1}W_T
\end{aligned}
$$

$$\underbrace{\phantom{X_0 = \mathrm{ReLU}(XW_0)}}_{\text{initial MLP layers}} \qquad\qquad \underbrace{\phantom{X_{T+1} = X_T + \gamma\bar{A}X_TW_T}}_{\text{scaled residual layers}}$$

$$
Y = \mathrm{softmax}(X_{T+L}W_{T+1}),
\tag{5}
$$

where $W_{T+1} \in \mathbb{R}^{h \times C}$.

With simple algebraic operations, (5) simplifies to the following model

$$
\begin{aligned}
X_0 &= \mathrm{ReLU}(XW_0) \\
X_1 &= \mathrm{ReLU}(X_0W_1) \\
&\ \ \vdots \\
X_T &= \mathrm{ReLU}(X_{T-1}W_{T-1})
\end{aligned}
$$

$$
Y = \mathrm{softmax}\left(\left(\left(X_T + \sum_{k=1}^{L-1} L\gamma^k\bar{A}^kX_TW_T^k + \gamma^L\bar{A}^LX_TW_T^L\right)W_{T+1}\right)\right).
\tag{6}
$$

We name the above models represented by both (5) and (6) *Graph Polynomial Convolution Network (GPCN)*.

It is easy to see that (6) has some similarity to GPR (2) with the sum of higher-orders of the normalized adjacency matrix. It is necessary to identify the main distinctive feature of (6) having higher-order of weights different from GPR (2). The higher-orders of the weight W_T may allow nonlinear mixing of weight parameters at each higher-order convolution compared to linear weight summation as in (3). Further, as we demonstrate later with theoretical analysis, higher-order weights allow the model to learn from smaller number of convolution avoiding oversmoothing. We propose to tune both T and L as hyperparameters.

3.2 Hybrid Model with Graph Topology

As we have indicated in the introduction some datasets can give an optimal performance by only learning from graph data with LINK. Hence, we propose to include an exclusive learning component from the adjacency matrix to the proposed models (5) and (6). A simple way to achieve this is by adding direct learning with the normalized adjacency

matrix and combining it to the graph convolution with a scaling of $\mu \in [0, 1]$ at the output layers of (5) and (6). With an additional weight $W_A \in \mathbb{R}^{N \times h}$ and learning μ as a parameter, we define GPCN-LINK as

$$
\begin{aligned}
X_0 &= \text{ReLU}(XW_0) & X_{T+1} &= X_T + \gamma \bar{A} X_T W_T \\
X_1 &= \text{ReLU}(X_0 W_1) & X_{T+2} &= X_{T+1} + \gamma \bar{A} X_{T+1} W_T \\
&\;\;\vdots & &\;\;\vdots \\
X_{T-1} &= \text{ReLU}(X_{T-2} W_{T-1}) & X_{T+L} &= X_{T+L-1} + \gamma \bar{A} X_{T+L-1} W_T \\
Y &= \text{softmax}((\mu X_{T+L} + (1-\mu)\bar{A} W_A) W_{T+1}).
\end{aligned}
\tag{7}
$$

Using similar simplification as in (6) to (7), we obtain

$$
\begin{aligned}
X_0 &= \text{ReLU}(XW_0) \\
X_1 &= \text{ReLU}(X_0 W_1) \\
&\;\;\vdots \\
X_T &= \text{ReLU}(X_{T-1} W_{T-1}) \\
Y &= \text{softmax}\left(\mu \left(X_T + \sum_{k=1}^{L-1} L \gamma^k \bar{A}^k X_T W_T^k + \gamma^L \bar{A}^L X_T W_T^L \right) + (1-\mu)\bar{A} W_A \right) W_{T+1} \right).
\end{aligned}
\tag{8}
$$

3.3 Adaptive Models

Instead of having a fixed scaling parameter γ for GPCN and GPCN-LINK, we propose to learn γ adaptively at each order of k. We can develop different strategies to learn γ adaptively as previously explored in GPRGNN Chien et al. (2021); Wimalawarne and Suzuki (2021). However, for simplicity we employ a simple way to make adaptive coefficients to have learnable parameters $\theta \in \mathbb{R}^{L+1}$ and apply L2-norm regularization. The resulting model is

$$
\begin{aligned}
X_0 &= \text{ReLU}(XW_0) \\
X_1 &= \text{ReLU}(X_0 W_1) \\
&\;\;\vdots \\
X_T &= \text{ReLU}(X_{T-1} W_{T-1}) \\
Y &= \text{softmax}\left(\left(\theta_0 X_T + \sum_{k=1}^{L} \theta_k \bar{A}^k X_T W_T^k \right) W_{T+1} \right).
\end{aligned}
\tag{9}
$$

We call the above model *Adaptive GPCN* (AGPCN). Further, we propose AGPCN-LINK by making both γ and μ in (8) adaptive.

4 Theoretical Analysis

We analyze generalization bounds of the proposed models using transductive Redemacher complexity El-Yaniv and Pechyony (2009); Oono and Suzuki (2020b) under the semi-supervised node classification setting similar to Wimalawarne and Suzuki (2021).

We recall that node feature matrix given by $X \in \mathbb{R}^{N \times q}$ and consider a 1-class labeled output by $Y \in \mathbb{R}^{N \times 1}$. Let us consider the sets $\mathcal{X}$ and $\mathcal{Y}$ such that $X \subseteq \mathcal{X}, Y \subseteq \mathcal{Y}$ and $(x_i, y_i) \in \mathcal{X} \times \mathcal{Y}$. We represent D_{train} and D_{test} as the training and test sets, respectively and samples are drawn without replacement for D_{train} and D_{test} such that $D_{\text{train}} \cup D_{\text{test}} = V$ and $D_{\text{train}} \cap D_{\text{test}} = \emptyset$. Further, we denote $M := |D_{\text{train}}|$ and $U := |D_{\text{test}}|$ and define $Q := 1/M + 1/U$. We also specify $C_0, \dots, C_L \in \mathbb{N}_+$ with $C_0 = q$, $C_1 = \dots = C_T = h$ and $C_{T+1} = 1$ to represent the dimensions of hidden layers and the output of proposed models.

We analyze the generalization bound for the model GPCN-LINK (8) from which we can derive the generalization bounds for other model. We define the hypothesis class for GPCN-LINK by

$$\mathcal{F}_{\mu,\gamma} = \Big\{ X, \bar{A} \mapsto \text{softmax}\Big(f^{(3)} \circ (\mu f^{(1)} \circ g^{(T)} \circ \cdots \circ g^{(0)}(X) + (1-\mu)f^{(2)}(\bar{A})) \Big| $$

$$g^{(l)}(Z) = \text{Relu}(ZW^{(l)}), f^{(1)}(X_T) = X_T + \sum_{k=1}^{L-1} L\gamma^k \bar{A}^k X_T W^{(T)k} + \gamma^L \bar{A}^L X_T W^{(T)L} \Big),$$

$$f^{(2)}(\bar{A})) = \bar{A} W^{(A)}, \ f^{(3)}(Z) = ZW^{(T+1)}, \ \|W^{(l)}_{\cdot c}\|_1 \le B^{(l)} \text{ for all } c \in [C_{l+1}], \|W^{(A)}_{\cdot c}\|_1 \le B^{(A)} \Big\}, \quad (10)$$

where use notation $W^{(l)} := W_l$ for (8), $W^{(l)} \in \mathbb{R}^{C_l \times C_{l+1}}$ $l = 0, \ldots, T-1$, $W^{(T+1)} := W_{T+1} \in \mathbb{R}^{C_{T+1} \times 1}$, $W^{(A)} := W_A \in \mathbb{R}^{N \times C_T}$, and $\sigma : \mathbb{R} \to \mathbb{R}$ is a 1-Lipschitz function such that $\sigma(0) = 0$ (e.g. ReLU with output clipping or a Sigmoid function) with bounded output as $|\sigma(\cdot)| \le R$, and $B^{(l)}$ $l = 0, \ldots, L$ are constants.

We consider a predictor $h : \mathcal{X} \to \mathcal{Y}$, $h \in \mathcal{F}_{\mu,\gamma}$ and a loss function $l(\cdot, \cdot)$ (e.g., Sigmoid, Sigmoid cross entropy). Now we define the training training error by $R(h) = \frac{1}{M} \sum_{n \in V_{\text{train}}} l(h(x_n), y_n)$ and test error by $\hat{R}(h) = \frac{1}{U} \sum_{n \in V_{\text{test}}} l(h(x_n), y_n)$. Using the standard approach in El-Yaniv and Pechyony (2009), we state the generalization bounds for transductive Rademacher complexity $\mathcal{R}(\mathcal{F}_{\mu,\gamma}, p)$ with $p \in [0, 0.5]$, $S := \frac{2(M+U)\min(M,U)}{(2(M+U)-1)(2\min(M,U)-1)}$, and probability $1 - \delta$ as

$$R(h) \le \hat{R}(h) + \mathcal{R}(\mathcal{F}_{\mu,\gamma}, p_0) + c_0 Q \sqrt{\min(M, U)} + \sqrt{\frac{SQ}{2} \log \frac{1}{\delta}}, \quad (11)$$

where

$$\mathcal{R}(\mathcal{V}, p) = Q \mathbb{E}_\epsilon \Big[\sup_{v \in \mathcal{V}} \langle \epsilon, v \rangle \Big],$$

where $\epsilon = (\epsilon_1, \ldots, \epsilon_N)$ is a sequence of i.i.d. Rademacher variables with distribution $\mathbb{P}(\epsilon_i = 1) = \mathbb{P}(\epsilon_i = -1) = p$ and $\mathbb{P}(\epsilon_i = 0) = 1 - 2p$ and c_0 is a constant. We consider the special case where $p = p_0 = MU/(M+U)^2$ as developed in Oono and Suzuki (2020b) to arrive at the desired generalization error bound. Using the above setting, we state the following two theorems for bounds Rademacher complexity of the GPCN-LINK and AGPCN-LINK.

Theorem 1. *The Rademacher complexity of the GPCN-LINK is bounded as*

$$Q^{-1} \bar{\mathcal{R}}(\tilde{\mathcal{H}}^{(0)}, p) \le C' B^{(T+1)} \mu \Big[2^T \prod_{l=0}^{T-1} B^{(l)} \sqrt{\frac{2MU}{(M+U)^2}} \Big(I + \sum_{k=1}^{L-1} B^{(T)k} L\gamma^k \sum_{j=1}^{N} |\lambda_j|^k $$

$$+ \gamma^L B^{(T)L} \sum_{j=1}^{N} |\lambda_j|^L \Big) \|X\|_F + \Big(\sum_{k=1}^{L-1} B^{(T)k} L\gamma^k \sum_{j=1}^{N} |\lambda_j|^k $$

$$+ \gamma^L B^{(T)L} \sum_{j=1}^{N} |\lambda_j|^L \Big) D \Big] + (1-\mu) 2^{5/2} \frac{B^{(T+1)} B^{(A)} \sqrt{MU}}{(M+U)} \sum_{i=1}^{N} |\lambda_i|.$$

where λ_i is the ith largest eigenvalue of $\tilde{A}$, $D = \sqrt{N}R$, and C' is a universal constant.

Theorem 2. *The Rademacher complexity of the AGPCN-LINK is bounded as*

$$\mathcal{R}(\mathcal{F}_{\mu,\gamma}, p_0) \le C' B^{(T+1)} \mu \Big[2^T \prod_{l=0}^{T-1} B^{(l)} \sqrt{\frac{2MU}{(M+U)^2}} \Big(\theta_0 I + \sum_{k=1}^{L} B^{(T)k} \theta_k \sum_{j=1}^{N} |\lambda_j|^k \Big) \prod_{l=0}^{T-1} B^{(l)} \|X\|_F $$

$$+ \Big(\sum_{k=1}^{L} B^{(T)k} \theta_k \sum_{j=1}^{N} |\lambda_j|^k \Big) D \Big] + (1-\mu) 2^{5/2} \frac{B^{(T+1)} B^{(A)} \sqrt{MU}}{(M+U)} \sum_{i=1}^{N} |\lambda_i|.$$

where λ_i is the ith largest eigenvalue of $\tilde{A}$, $D = \sqrt{N}R$, and C' is a universal constant.

By setting $\mu = 1$. we obtain bounds for GPCN and AGPCN from Theorem 1 and Theorem 2, respectively. Similar to the analysis in Wimalawarne and Suzuki (2021), since the normalized adjacency matrix has a eigenvalue spectrum of $1 = \lambda_1 \ge \lambda_2 \ge \cdots \ge \lambda_N \ge -1$, as the residual layers (k) increases the summation of eigenvalues becomes small.

Method	Chameleon	Squirrel	Film/Actor	Cornell	Texas	Wisconsin
Classes	5	5	5	5	5	5
Nodes	2277	5201	7600	183	183	251
Edges	36101	198353	29926	295	309	499
Features	2089	2325	931	1703	1703	1703
Edge Homoph.	0.247	0.215	0.22	0.301	0.057	0.21
Homophily	0.062	0.025	0.011	0.047	0.001	0.094
MLP	47.89±2.56	30.10±2.00	**37.38±0.85**	**84.86±6.85**	79.18±6.28	81.17±5.96
GCN	61.18±2.74	46.23±2.62	27.61±0.95	58.64±5.54	58.92±5.24	48.43±4.88
SGC	63.61±2.55	43.71±1.69	27.42±1.16	57.02±5.85	58.64 ±5.92	49.21±3.44
GPRGNN	65.76±1.57	51.19±1.41	35.46±0.92	**82.43±7.47**	**87.56±1.41**	85.88±4.09
H2GCN	57.11±1.58	36.42±1.89	35.86±1.03	**82.16±4.80**	**84.86±6.77**	**86.67±4.69**
MixHop	60.50±2.53	43.80±1.48	32.22±2.34	73.51±6.34	77.84±7.73	**85.88±4.22**
LINK	**72.01±1.37**	62.69±1.69	25.24±1.12	58.37±3.86	58.91±4.32	48.03±6.63
LINKX	68.42±1.38	61.81±1.80	36.10±1.55	77.84±5.81	74.60±8.37	75.49±5.72
GPCN	**71.40±1.56**	**64.30±2.24**	**36.77±1.10**	81.62±6.70	79.45±6.30	85.68±4.88
GPCN-LINK	**71.34±3.82**	**67.22±1.37**	**37.16±0.63**	66.21±6.42	67.29±9.85	65.29±14.19
AGPCN	67.12±2.51	58.16±1.63	36.13±1.04	80.0±6.41	**80.81±5.04**	**86.47±4.42**
AGPCN-LINK	71.07±1.81	**65.61±2.96**	36.46±1.03	64.86±8.28	66.21±9.06	68.23±13.66

Table 2: Node-classification accuracy of non-homophilous datasets from Pei et al. (2020). The best three results are highlighted.

Further, due to the polynomial structure of GPCN and GPCN-LINK, when $\gamma < 1$ and $B^{(T)} < 1$ as the residual layers increase their higher-powers shrink quickly. Hence, models with small number of residual layers would give a better generalization since the effect of very high orders of convolutions are redundant. When $\gamma > 1$ or $B^{(T)} > 1$, higher-order convolutions may get more prominent, then the bound can be too large. Moreover, it may result in summation of many fast shrinking powers of eigenvalues which lead to oversmoothing Oono and Suzuki (2020a). Again, oversmoothing can be avoided by selection of smaller number of residual layers. Furthermore, if μ is very small then models learn mainly by direct learning from the adjacency matrix with limited contribution from graph convolution, leading to less oversmoothing. Similar arguments apply for AGPCN and AGPCN-LINK where the models need to learn θ to avoid oversmoothing by using appropriate levels of higher orders convolutions.

5 Related Methods

Convolution by higher-orders of the normalized adjacency matrix has been employed by several graph convolution models such as GPRGNN Chien et al. (2021), MixHop Abu-El-Haija et al. (2019), AdaGPR Wimalawarne and Suzuki (2021), and H2GCN Zhu et al. (2020). All these methods have shown that higher-order convolutions can obtain higher accuracy for non-homophilous graphs compared models that apply convolution by a single adjacency matrix. GPCN and their variations differ from all the previous models since it uses higher powers of weight matrices that constructs a polynomial structure for graph convolution. Furthermore, GPCN-LINK and AGPCN-LINK also employ learning directly from the adjacency matrix allowing adaptive decoupled learning from graph convolution and graph data. Hence, our proposed methods are significantly different from existing graph convolution models that uses higher-order convolutions.

The use of direct learning from the adjacency matrix in GPCN-LINK and APGCN-LINK was inspired by the LINK and LINKX. However, both LINKX Lim et al. (2021a) and LINK Zheleva and Getoor (2009) have no graph convolution on node features. Furthermore, we propose to have adaptive scaling between graph convolution and direct learning from adjacency matrix, which makes our methods considerable different from LINK and LINKX.

6 Experiments

We conducted node classification experiments to evaluate the proposed methods using non-homophilous graphs. First, we consider non-homophilous graphs Chameleon, Squirrel, Cornell, Texas, and Wisconsin from Pei et al. (2020). We used their original data splittings, which randomly split into training, validation and testing sets with nodes from each class with percentages of 60%, 20%, and 20%, respectively. Further, we use directed graphs of these datasets as originally used by Pei et al. (2020). Additionally, we experimented with selected datasets from the recently introduced non-homophilous graphs from Lim et al. (2021b,a). Due to computational limitations, we only used five datasets with

Method	Twitch-DE	Penn94	Yelp-Chi	Deezer-europe	Genius
Classes	2	2	2	2	2
Nodes	9498	41,554	45,954	28,281	421,961
Edges	153138	1,362,803	3,846,979	92,752	984,979
Features	2545	5	32	31,241	12
Edge Homoph.	0.632	0.470	0.773	0.525	0.618
Homophily	0.146	0.046	0.052	0.030	0.090
MLP	$69.20\pm_{0.62}$	$73.61\pm_{0.40}$	$\mathbf{87.94\pm_{0.52}}$	$66.55\pm_{0.72}$	$86.68\pm_{0.09}$
GCN	$\mathbf{74.07\pm_{0.68}}$	$82.47\pm_{0.27}$	$63.62\pm_{1.00}$	$62.23\pm_{0.53}$	$87.42\pm_{0.37}$
SGC	$72.30\pm_{0.22}$	$66.79\pm_{0.27}$	$58.62\pm_{0.85}$	$59.73\pm_{0.12}$	$82.36\pm_{0.37}$
GPRGNN	$\mathbf{73.84\pm_{0.69}}$	$84.59\pm_{0.29}$	$86.57\pm_{0.89}$	$\mathbf{66.90\pm_{0.50}}$	$90.05\pm_{0.31}$
H2GCN	$72.67\pm_{0.65}$	(M)	$\mathbf{88.48\pm_{0.21}}$	$67.22\pm_{0.90}$	(M)
MixHop	$73.23\pm_{0.99}$	$83.47\pm_{0.71}$	$\mathbf{87.02\pm_{0.50}}$	$67.80\pm_{0.58}$	$90.58\pm_{0.09}$
LINK	$72.42\pm_{0.57}$	$80.79\pm_{0.03}$	$63.44\pm_{1.07}$	$57.71\pm_{0.36}$	$72.58\pm_{0.14}$
LINKX	$72.64\pm_{0.89}$	$84.71\pm_{0.52}$	$76.84\pm_{1.82}$	$66.11\pm_{0.70}$	$90.77\pm_{0.27}$
GPCN	$\mathbf{73.79\pm_{0.81}}$	$\mathbf{84.93\pm_{0.32}}$	$85.86\pm_{0.52}$	$64.21\pm_{1.43}$	$90.53\pm_{0.05}$
GPCN-LINK	$73.51\pm_{0.73}$	$\mathbf{86.16\pm_{0.26}}$	$86.48\pm_{0.63}$	$65.69\pm_{0.74}$	$\mathbf{90.98\pm_{0.01}}$
AGPCN	$73.66\pm_{0.65}$	$84.73\pm_{0.32}$	$85.88\pm_{0.83}$	$66.39\pm_{0.51}$	$\mathbf{91.79\pm_{0.06}}$
AGPCN-LINK	$73.41\pm_{0.52}$	$\mathbf{86.28\pm_{0.20}}$	$86.22\pm_{0.22}$	$66.06\pm_{0.37}$	$\mathbf{91.74\pm_{0.19}}$

Table 3: Node-classification accuracy of non-homophilous datasets from Lim et al. (2021a,b). The best three results are highlighted.

nodes less than 50000, which include Penn94 Traud et al. (2012), twitch-gamer Rozemberczki and Sarkar (2021), deezer-europe Rozemberczki and Sarkar (2020), and yelp-chi Mukherjee et al. (2021). For these datasets we used the 5 data splits based on train/validation/test sampling of 0.5/0.25/0.25 as used in Lim et al. (2021b,a).

We performed hyperparameter tuning for the proposed models with hidden $\in \{64, 512\}$, learning parameter $\in \{0.01, 0.05\}$, weight decay $\in \{0.0, 0.001, 0.00001\}$, initial feature learning layers $\in \{1, 2, 3, 4, 5\}$, residual layers $(L) \in \{1, 2, 4, 8\}$, $\gamma \in \{2^8, 2^6, \dots, 2^0, 2^{-2}, \dots, 2^{-6}\}$, and dropout $\in \{0, 0.3, 0.6, 0.9\}$. For all our experiments we used NVidia GPU V100-PCIE-16GB environment hosted on Intel Xeon Gold 6136 processor servers. A Pytorch implementation of GPCN is available at https://github.com/kishanwn/GPCN.

As baseline methods, we considered MLP, GCN Kipf and Welling (2017) ,SGC Wu et al. (2019), GPRGNN Chien et al. (2021), H2GCN Zhu et al. (2020), MixHop Abu-El-Haija et al. (2019), LINKZheleva and Getoor (2009), and LINKX Lim et al. (2021b). Due to the use of same data splittings we borrowed node classification results for baseline methods from Lim et al. (2021b,a). Since we could not find results with LINK for datasets from Pei et al. (2020) and LINKX results for Deezer-europe, Twitch-DE, and Yelp-chi, we performed their experiments using the same hyperparameter settings specified in Lim et al. (2021a). We provide further experiment with homophilous graphs and ablation studies in Section C and Section D of the appendix.

Table 2 shows the accuracy for non-homophilous datasets from Pei et al. (2020). An important observation we want to highlight is the high accuracy obtained by LINK for Chameleon and Squirrel compared to well-known graph convolution models. MLP has given the lowest accuracy for these two datasets. This indicates that the adjacency matrix contains important features for learning compared to node features. GPCN and GPCN-LINK have given significant improvements for Squirrel and a comparable accuracy compared to LINK for Chameleon. For Film dataset, MLP has given the best performance indicating the node features are more important than graph information, here again, GPCN and GPCN-LINK have given comparable accuracies to MLP. An interesting observation is that only AGPCN has only given a comparable performance for Wisconsin among the small scale graphs.

Finally, table 3 shows results for the new non-homophilous datasets introduced by Lim et al. (2021b,a). GPCN-LINK and AGPCN-LINK have given have given significant accuracy for Penn94 and Genius compared to all the baseline methods. GPCN has obtained a comparable performance for Twitch-DE with GPCN. For both Yelp-chi and Deezer-Europe, our proposed methods have obtained comparable performance against GPRGNN, however, they have recorded less accuracy compared to H2GCN and MixHop. We further emphasize that AGPCN provide comparable accuracy with GPRGNN for all datasets in table 3. Furthermore, we want to point out that overall our methods have obtained improved accuracy compared to LINKX and LINK.

7 Conclusions and Future Research

We propose a new class of graph convolution models that consists of a polynomial of normalized adjacency matrix and weight matrices. We provided multiple levels of adaptive learning for higher-order graph convolution and direct learning from adjacency matrices. Using theoretical analysis, we demonstrate that our methods are able to obtain better generalization bounds by avoiding unnecessary higher-order convolution and by mixed learning of graph convolution and direct learning from adjacency matrices. By experiments with non-homophilous graphs we demonstrated that our proposed methods can obtained improved performance for node classification compared to many state of the art graph convolution models.

A useful possible extension of the GPCN is to develop generalized polynomial convolution models where residual layers have different weights. Further research in the direction of adaptive learning may help to reduce the considerable number of hyperparameters.

8 Societal Impacts and Limitations

Node classification is important application in multiple domains. Further, there are many real-world domains with non-homophilous graphs. However, learning on node features and graph topology may lead to violation of privacy of individuals. A potential practical limitation of the proposed is the considerable number of hyperparameters that needs to be tuned.

References

Abu-El-Haija, S., Perozzi, B., Kapoor, A., Alipourfard, N., Lerman, K., Harutyunyan, H., Steeg, G. V., and Galstyan, A. (2019). MixHop: Higher-order graph convolutional architectures via sparsified neighborhood mixing. In *ICML*. PMLR.

Adamczak, R. (2015). A note on the hanson-wright inequality for random vectors with dependencies. *Electronic Communications in Probability*, 20:1–13.

Chien, E., Peng, J., Li, P., and Milenkovic, O. (2021). Adaptive universal generalized pagerank graph neural network. In *ICLR*.

El-Yaniv, R. and Pechyony, D. (2009). Transductive rademacher complexity and its applications. *J. Artif. Int. Res.*, page 193–234.

Kipf, T. N. and Welling, M. (2017). Semi-Supervised Classification with Graph Convolutional Networks. In *ICLR*, ICLR '17.

Li, C. and Goldwasser, D. (2019). Encoding social information with graph convolutional networks for Political perspective detection in news media. In *ACL*.

Lim, D., Hohne, F. M., Li, X., Huang, S. L., Gupta, V., Bhalerao, O. P., and Lim, S.-N. (2021a). Large scale learning on non-homophilous graphs: New benchmarks and strong simple methods. In *NeurIPS*.

Lim, D., Li, X., Hohne, F., and Lim, S.-N. (2021b). New benchmarks for learning on non-homophilous graphs. *Workshop on Graph Learning Benchmarks, WWW 2021*.

McPherson, M., Smith-Lovin, L., and Cook, J. M. (2001). Birds of a feather: Homophily in social networks. *Annual Review of Sociology*.

Mukherjee, A., Venkataraman, V., Liu, B., and Glance, N. (2021). What yelp fake review filter might be doing? *ICWSM*.

Oono, K. and Suzuki, T. (2020a). Graph neural networks exponentially lose expressive power for node classification. In *ICLR 2020*.

Oono, K. and Suzuki, T. (2020b). Optimization and generalization analysis of transduction through gradient boosting and application to multi-scale graph neural networks. In *NeurIPS 2020*.

Pei, H., Wei, B., Chang, K. C., Lei, Y., and Yang, B. (2020). Geom-gcn: Geometric graph convolutional networks. In *ICLR 2020*, ICLR'20.

Poli, M., Massaroli, S., Park, J., Yamashita, A., Asama, H., and Park, J. (2019). Graph neural ordinary differential equations. *arXiv preprint arXiv:1911.07532*.

Rozemberczki, B. and Sarkar, R. (2020). Characteristic Functions on Graphs: Birds of a Feather, from Statistical Descriptors to Parametric Models. In *CIKM '20*.

Rozemberczki, B. and Sarkar, R. (2021). Twitch gamers: a dataset for evaluating proximity preserving and structural role-based node embeddings. *CoRR*, abs/2101.03091.

Schlichtkrull, M., Kipf, T. N., Bloem, P., van den Berg, R., Titov, I., and Welling, M. (2018). Modeling relational data with graph convolutional networks. In *The Semantic Web*.

Traud, A. L., Mucha, P. J., and Porter, M. A. (2012). Social structure of Facebook networks. *Physica A: Statistical Mechanics and its Applications*, 391(16):4165–4180.

Wimalawarne, K. and Suzuki, T. (2021). Adaptive and interpretable graph convolution networks using generalized pagerank. *CoRR*.

Wu, F., Souza, A., Zhang, T., Fifty, C., Yu, T., and Weinberger, K. (2019). Simplifying graph convolutional networks. In *ICML*.

Ying, R., He, R., Chen, K., Eksombatchai, P., Hamilton, W. L., and Leskovec, J. (2018). Graph convolutional neural networks for web-scale recommender systems. In *KDD '18*.

Zhao, L., Peng, X., Tian, Y., Kapadia, M., and Metaxas, D. N. (2019). Semantic graph convolutional networks for 3d human pose regression. In *(CVPR)*.

Zheleva, E. and Getoor, L. (2009). To join or not to join: The illusion of privacy in social networks with mixed public and private user profiles. WWW '09.

Zhu, J., Yan, Y., Zhao, L., Heimann, M., Akoglu, L., and Koutra, D. (2020). Beyond homophily in graph neural networks: Current limitations and effective designs. *NeurIPS*.

A   Generalized Polynomial Model

For completeness, we provide the model of removing ReLU activations from the scaled residual layers having different weight matrices, which leads to the generalized polynomial model. The resulting extention to (4) is

$$
\begin{aligned}
X_0 &= XW_0 \\
X_1 &= X_0 + \gamma \bar{A} X_0 W_1 \\
X_2 &= X_1 + \gamma \bar{A} X_1 W_2 \\
&\vdots \\
X_L &= X_{L-1} + \gamma \bar{A} X_{L-1} W_L \\
Y &= \text{sigmoid}(X_{L+1} W_2),
\end{aligned}
$$

which leads a generalized polynomial model of

$$
Y = \text{sigmoid}\Bigg(\Big(XW_0 + \gamma \bar{A}(XW_0)(W_1 + \cdots + W_L) + \gamma^2 \bar{A}^2(XW_0)(W_1 W_2 + \cdots + W_1 W_L) \\
+ \cdots \gamma^k \bar{A}^k (XW_0) W_1 W_2 \cdots W_L \Big) W_{L+1}\Bigg).
$$

It is easy to see that above models reduces to GPCN models if the same weight is applied to each residual layer. We propose the study of the generalized polynomial convolution models as a future research direction.

B   Proof of Theoretical Results

We state the transductive Rademacher complexity El-Yaniv and Pechyony (2009) in the following definition.

Definition 1. *Given $p \in [0, 0.5]$ and $\mathcal{V} \subset \mathbb{R}^N$, the transductive Rademacher complexity is defined as*

$$
\mathcal{R}(\mathcal{V}, p) = Q \mathbb{E}_\epsilon \left[\sup_{v \in \mathcal{V}} \langle \epsilon, v \rangle \right],
$$

where $Q = \frac{1}{M} + \frac{1}{N}$ and $\epsilon = (\epsilon_1, \ldots, \epsilon_N)$ is a sequence of i.i.d. Rademacher variables with distribution $\mathbb{P}(\epsilon_i = 1) = \mathbb{P}(\epsilon_i = -1) = p$ and $\mathbb{P}(\epsilon_i = 0) = 1 - 2p$.

We borrow the following symmetric Rademacher complexity from Oono and Suzuki (2020b), which is a variant of the tranductive Rademacher complexity in Definition 1.

Definition 2. *Given $p \in [0, 0.5]$ and $\mathcal{V} \subset \mathbb{R}^N$, the symmetric transductive Rademacher complexity is defined as*

$$
\bar{\mathcal{R}}(\mathcal{V}, p) = Q \mathbb{E}_\epsilon \left[\sup_{v \in \mathcal{V}} |\langle \epsilon, v \rangle| \right],
$$

where $Q = \frac{1}{M} + \frac{1}{N}$ and $\epsilon = (\epsilon_1, \ldots, \epsilon_N)$ is a sequence of i.i.d. Rademacher variables with distribution $\mathbb{P}(\epsilon_i = 1) = \mathbb{P}(\epsilon_i = -1) = p$ and $\mathbb{P}(\epsilon_i = 0) = 1 - 2p$.

Proof of Theorem 1. From Oono and Suzuki (2020b), it si known that $\mathcal{R}(\mathcal{F}, p) \leq \bar{\mathcal{R}}(\mathcal{F}, p)$. Hence, we bound (11) using the symmetric Rademacher complexity. We give the bound for a general p but the final bound can be obtained by substituting $p \leftarrow p_0$.

We use the abbreviation for the row s of any matrix Z by $Z_s := Z[s,:]$, columns c by $Z_{\cdot c} := X[:,c]$, and an element by $Z_{sc} := Z[s,c]$. We decompose the hyperthesis class in (10) into several components as

$$\mathcal{G}^{(0)} = \left\{ \sum_{c=1}^{C_0} X_{\cdot c} w_c^{(0)} \Big| \|w_c^{(0)}\|_1 \leq B^{(0)} \right\},$$

$$\tilde{\mathcal{G}}^{(0)} = \sigma \circ \mathcal{G}^{(0)},$$

$$\mathcal{G}^{(l)} = \left\{ \sum_{c=1}^{C_l} Z_{\cdot c} w_c^{(l)} \Big| \|w_c^{(l)}\|_1 \leq B^{(l)}, Z \in \mathcal{G}^{(l-1)} \right\},$$

$$\tilde{\mathcal{G}}^{(l)} = \sigma \circ \mathcal{G}^{(l)}, \ l = 1, \ldots, T-1,$$

$$\mathcal{H}^{(0)} = \left\{ G + \sum_{k=1}^{L-1} \sum_{c=1}^{C_T} K \gamma^k [\bar{A}^k G]_{\cdot c} w_c^{(T)k} + \sum_{c=1}^{C_T} \gamma^K [\bar{A} G]_{\cdot c} w_c^{(T)k} \Big| G \in \tilde{\mathcal{G}}^{(T)}, \|w_c^{(T)}\|_1 \leq B^{(T)} \right\},$$

$$\tilde{\mathcal{H}}^{(0)} = \sigma \circ \mathcal{H}^{(0)}$$

$$\mathcal{H}^{(1)} = \left\{ \bar{A}_{\cdot c} w_c^{(A)} \Big| \|w_c^{(A)}\|_1 \leq B^{(A)} \right\}. \tag{12}$$

Now, let us consider the output layer, then

$$Q^{-1} \bar{\mathcal{R}}(\tilde{\mathcal{F}}_{\mu,\gamma}, p) = \mathbb{E}_{\epsilon} \left[\sup_{\|w_c^{(T+1)}\|_1 \leq B^{(T+1)}, Z^{(0)} \in \mathcal{H}^{(0)}, Z^{(1)} \in \tilde{\mathcal{H}}^{(1)}} \left| \sum_{n=1}^{N} \epsilon_n \sum_{c=1}^{C_{T+1}} \left(\mu Z_{nc}^{(0)} + (1-\mu) Z_{nc}^{(1)} \right) w_c^{(T+1)} \right| \right]$$

$$= \mathbb{E}_{\epsilon} \left[\sup_{\|w_c^{(T+1)}\|_1 \leq B^{(T+1)}, Z^{(0)} \in \mathcal{H}^{(0)}, Z^{(1)} \in \tilde{\mathcal{H}}^{(1)}} \left| \sum_{c=1}^{C_{L+1}} \sum_{n=1}^{N} \epsilon_n \left(\mu Z_{nc}^{(0)} + (1-\mu) Z_{nc}^{(1)} \right) w_c^{(T+1)} \right| \right]$$

$$\leq B^{(T+1)} \mathbb{E}_{\epsilon} \left[\sup_{Z^{(0)} \in \mathcal{H}^{(0)}, Z^{(1)} \in \tilde{\mathcal{H}}^{(1)}} \left| \sum_{n=1}^{N} \epsilon_n \left(\mu Z_n^{(0)} + (1-\mu) Z_n^{(1)} \right) \right| \right]$$

$$= B^{(T+1)} \mathbb{E}_{\epsilon} \left[\sup_{\|w_c^{(T)}\|_1 \leq B^{(T)}, \|w_c^{(A)}\|_1 \leq B^{(A)}, G \in \mathcal{G}^{(T-1)}} \right|$$

$$\sum_{n=1}^{N} \epsilon_n \left(\mu \left(G_n + \sum_{k=1}^{L-1} \sum_{c=1}^{C_{L+1}} K \gamma^k [\bar{A}^k G]_{nc} w_c^{(T)k} + \sum_{c=1}^{C_{L+1}} \gamma^K [\bar{A}^K G]_{nc} w_c^{(T)k} \right) \right. \tag{13}$$

$$\left. + (1-\mu) \sum_{c=1}^{C_{L+1}} \bar{A}_{nc} w_c^{(A)} \right) \Big| \right]$$

$$\leq B^{(L+1)} \mathbb{E}_{\epsilon} \left[\mu \sup_{\|w_c^{(T)}\|_1 \leq B^{(T)}, G \in \mathcal{G}^{(T-1)}} \left| \sum_{n=1}^{N} \epsilon_n \left(G_n + \sum_{k=1}^{L-1} \sum_{c=1}^{C_{L+1}} K \gamma^k [\bar{A}^k G]_{nc} w_c^{(T)k} \right. \right. \right.$$

$$\left. \left. + \sum_{c=1}^{C_{L+1}} \gamma^K [\bar{A}^K G]_{nc} w_c^{(T)k} \right) \right|$$

$$+ (1-\mu) \sup_{\|w_c^{(A)}\|_1 \leq B^{(A)}, G \in \mathcal{G}^{(T-1)}} \left| \sum_{n=1}^{N} \epsilon_n \sum_{c=1}^{C_{L+1}} \bar{A}_{nc} w_c^{(A)} \right| \right]$$

$$Q^{-1}\bar{\mathcal{R}}(\tilde{\mathcal{F}}_{\mu,\gamma},p) \le B^{(T+1)}\mathbb{E}_{\boldsymbol{\epsilon}}\left[\mu \sup_{\|w_c^{(T)}\|_1 \le B^{(T)}, G \in \mathcal{G}^{(T-1)}} \left|\sum_{n=1}^{N} \epsilon_n G_n\right|\right.$$

$$+ \left|\sum_{c=1}^{C_{L+1}} \sum_{k=1}^{L-1} \sum_{n=1}^{N} \epsilon_n K\gamma^k[\bar{A}^k G]_{nc} w_c^{(T)k}\right| + \left|\sum_{c=1}^{C_T} \sum_{n=1}^{N} \epsilon_n \gamma^K[\bar{A}^K G]_{nc} w_c^{(T)k}\right|$$

$$\left. + (1-\mu) \sup_{\|w_c^{(A)}\|_1 \le B^{(A)}} \left|\sum_{c=1}^{C_{L+1}} \left(\sum_{n=1}^{N} \epsilon_n \bar{A}_{nc}\right) w_c^{(A)}\right|\right] \tag{14}$$

$$\le B^{(T+1)}\mathbb{E}_{\boldsymbol{\epsilon}} \sup_{G \in \mathcal{G}^{(T-1)}} \left[\left|\sum_{n=1}^{N} \epsilon_n G_n\right| + \sum_{k=1}^{K-1} B^{(T)k} K\gamma^k \left|\sum_{n=1}^{N} \epsilon_n [\bar{A}^k G]_n\right|\right.$$

$$\left. + \gamma^K B^{(T)K} \left|\sum_{n=1}^{N} \epsilon_n [\bar{A}^K G]_n\right|\right] + (1-\mu)B^{(T+1)}B^{(A)}\mathbb{E}_{\boldsymbol{\epsilon}} \left|\left(\sum_{n=1}^{N} \epsilon_n \bar{A}_n\right)\right|,$$

where we have used the inequality $\|W_c^{(T)k}\|_1 \le \|W_c^{(T)}\|_1^k \le B^{(T)k}$.

Next, we reduce each component with expectation over ϵ in (14). Hence, we consider the bound of the term

$$\Pi = \mathbb{E}_{\boldsymbol{\epsilon}} \sup_{G \in \mathcal{G}^{(T-1)}} \left|\sum_{n=1}^{N} \epsilon_n [\bar{A}^k G]_n\right|. \tag{15}$$

Let $\epsilon' = (\epsilon_1', \ldots, \epsilon_N')$ be a random variable that is independent to and has the identical distribution as ϵ. Then, using a similar methods as in Wimalawarne and Suzuki (2021) we have that

$$\Pi = \mathbb{E}_{\epsilon}\left[\sup_{G \in \mathcal{G}^{(T-1)}} \left|\sum_{n=1}^{N} \epsilon_n[\tilde{A}^k \frac{1}{2p}\mathbb{E}_{\epsilon'}[\epsilon'\epsilon'^{\top}]G]_n\right|\right] \quad (\because \mathbb{E}_{\epsilon'}[\epsilon'\epsilon'^{\top}] = 2pI)$$

$$\le \frac{1}{2p}\mathbb{E}_{\epsilon,\epsilon'}\left[\sup_{G \in \mathcal{G}^{(T-1)}} \left|\epsilon^{\top}\tilde{A}^k\epsilon'\epsilon'^{\top}G\right|\right] \le \frac{1}{2p}\mathbb{E}_{\epsilon,\epsilon'}\left[\left|\epsilon^{\top}\tilde{A}^k\epsilon'\right| \sup_{G \in \mathcal{G}^{(T-1)}} \left|\epsilon'^{\top}G\right|\right]$$

$$= \frac{1}{2p}\mathbb{E}_{\epsilon'}\left[\mathbb{E}_{\epsilon}\left[\left|\epsilon^{\top}\tilde{A}^k\epsilon'\right|\right] \sup_{G \in \mathcal{G}^{(T-1)}} \left|\epsilon'^{\top}G\right|\right]$$

$$\le \frac{1}{2p}\mathbb{E}_{\epsilon'}\left[\sqrt{\mathbb{E}_{\epsilon}\left[\left(\epsilon^{\top}\tilde{A}^k\epsilon'\right)^2\right]} \sup_{G \in \mathcal{G}^{(T-1)}} \left|\epsilon'^{\top}G\right|\right]$$

$$= \frac{1}{2p}\mathbb{E}_{\epsilon'}\left[\sqrt{\mathbb{E}_{\epsilon}\left[\epsilon'^{\top}\tilde{A}^k\epsilon\epsilon^{\top}\tilde{A}^k\epsilon'\right]} \sup_{G \in \mathcal{G}^{(T-1)}} \left|\epsilon'^{\top}G\right|\right]$$

$$= \mathbb{E}_{\epsilon'}\left[\sqrt{\epsilon'^{\top}\tilde{A}^{2k}\epsilon'} \sup_{G \in \mathcal{G}^{(T-1)}} \left|\epsilon'^{\top}G\right|\right],$$

where we used $\mathbb{E}_{\epsilon}[\epsilon\epsilon^{\top}] = 2pI$ in the last equation. Again, as in Wimalawarne and Suzuki (2021) we use Hanson-Wright concentration inequality (Theorem 2.5 of Adamczak (2015)), which results in

$$\mathbb{P}[|\epsilon'^{\top}\tilde{A}^{2k}\epsilon' - \mathbb{E}_{\epsilon'}[\epsilon'^{\top}\tilde{A}^{2k}\epsilon']| \ge c(\sqrt{2p}\|\tilde{A}^{2k}\|_F\sqrt{t} + \|\tilde{A}^{2k}\|t)] \le \exp(-t) \quad (t > 0),$$

with a universal constant c, where $\|A\|_F = \sqrt{\text{Tr}[AA^{\top}]}$. Further, the Talagrand's concentration inequality yields

$$\mathbb{P}\left[\left|\sup_{G \in \mathcal{G}^{(T-1)}} \epsilon'^{\top}G\right| \ge c'\left(\mathbb{E}_{\epsilon'}\left[\sup_{G \in \mathcal{G}^{(T-1)}} \left|\epsilon'^{\top}G\right|\right]\right.\right.$$

$$\left.\left. + \sqrt{Nt \sup_{G \in \mathcal{G}^{(T-1)}} \sum_{n=1}^{N} G_n^2/N + t \sup_{G \in \mathcal{G}^{(T-1)}} \|G\|_{\infty}}\right)\right] \le e^{-t} \quad (t > 0), \tag{16}$$

where $c' > 0$ is a universal constant. Then, by noticing that $\mathbb{E}_{\epsilon'}[\epsilon'^\top A \epsilon'] = 2p\mathrm{Tr}[A]$, these inequalities yield

$$
\mathbb{E}_{\epsilon'}\left[\sqrt{\epsilon'^\top \tilde{A}^{2k}\epsilon'} \sup_{G \in \mathcal{G}^{(T-1)}} |\epsilon'^\top G|\right]
$$
$$
\leq \int \sqrt{2p\mathrm{Tr}[\tilde{A}^{2k}] + c(\sqrt{2p}\|\tilde{A}^{2k}\|_F \sqrt{t} + \|\tilde{A}^{2k}\|t)}
$$
$$
c'(|\mathbb{E}_{\epsilon'} \sup_{G \in \mathcal{G}^{(T-1)}} \epsilon'^\top G| + \sqrt{t}\|\mathcal{H}^{(l)}\|_2 + t\|\mathcal{H}^{(l)}\|_\infty)2\exp(-t)\mathrm{d}t
$$

where we define $\|\mathcal{H}^{(l)}\|_* := \sup_{G \in \mathcal{G}^{(T-1)}} \|G\|_*$ for $* = 2$ and ∞. This leads to the right hand bound as $C\sqrt{\mathrm{Tr}[\tilde{A}^{2k}]}\left(\mathbb{E}_{\epsilon'}\left[\sup_{G \in \mathcal{G}^{(T-1)}} |\epsilon'^\top G|\right] + \|\mathcal{H}^{(l)}\|_2\right)$ for a universal constant C, where we used $2p \leq 1$. using the assumption that the output is bounded by the activation function, we take $\sup_{Z \in \mathcal{H}^{(l)}} \|Z\|_2 \leq \sqrt{N}R =: D$. Now, we have

$$
\Pi \leq \left[C\sqrt{\mathrm{Tr}[\tilde{A}^{2k}]}\left(\mathbb{E}_\epsilon \sup_{G \in \mathcal{G}^{(T-1)}} \left|\sum_{n=1}^N \epsilon_n G_n\right| + D\right)\right]
$$
$$
\leq \left[C\sqrt{\left(\sum_{i=1}^N \lambda_i^k\right)^2}\left(\mathbb{E}_\epsilon \sup_{G \in \mathcal{G}^{(T-1)}} \left|\sum_{n=1}^N \epsilon_n G_n\right| + D\right)\right]
$$
$$
\leq \left[C\sum_{i=1}^N |\lambda_i|^k\left(\mathbb{E}_\epsilon \sup_{G \in \mathcal{G}^{(T-1)}} \left|\sum_{n=1}^N \epsilon_n G_n\right| + D\right)\right]. \tag{17}
$$

Further, we can bound the last term of (14) by

$$
R.H.S = (1-\mu)B^{(T+1)}B^{(A)}\mathbb{E}_\epsilon\left[\sup\left|\sum_{n=1}^N \epsilon_n \bar{A}_n\right|\right]
$$
$$
\leq 2(1-\mu)B^{(T+1)}B^{(A)}\mathbb{E}_\epsilon\left[\left\|\sum_{n=1}^N \epsilon_n \bar{A}_{n\cdot}\right\|_2\right]
$$
$$
\leq 2(1-\mu)B^{(T+1)}B^{(A)}\sqrt{\mathbb{E}_\epsilon \sum_{c=1}^{C_0}\left(\sum_{n=1}^N \epsilon_n \bar{A}_{nc}\right)^2} \quad \text{(Jensen Inequality)}
$$
$$
= 2(1-\mu)B^{(T+1)}B^{(A)}\sqrt{\mathbb{E}_\epsilon \sum_{c=1}^{C_0}\sum_{n,m=1}^N \epsilon_n \epsilon_m \bar{A}_{nc}\bar{A}_{mc}}
$$
$$
= 2(1-\mu)B^{(T+1)}B^{(A)}\sqrt{\sum_{c=1}^{C_0}\sum_{m=1}^N 2p(\bar{A}_{mc})^2}
$$
$$
= 2(1-\mu)B^{(T+1)}B^{(A)}\sqrt{2p}\|\bar{A}\|_F
$$
$$
\leq 2(1-\mu)B^{(T+1)}B^{(A)}\sqrt{2p}\sum_{i=1}^N |\lambda_i|.
$$

Uisng the assumption that $p = p_0 = \frac{MU}{(M+U)^2}$, we have

$$
R.H.S \leq 2^{5/2}(1-\mu)\frac{B^{(T+1)}B^{(A)}\sqrt{MU}}{(M+U)}\sum_{i=1}^N |\lambda_i|. \tag{18}
$$

Now applying (17) and (18) to (14) for $p = p_0$, we have

$$Q^{-1}\bar{\mathcal{R}}(\tilde{\mathcal{F}}_{\mu,\gamma}, p_0)C \leq B^{(T+1)}\mu\left[\left(I + \sum_{k=1}^{L-1} B^{(T)k}K\gamma^k \sum_{j=1}^{N}|\lambda_j|^k + \gamma^L B^{(T)L}\sum_{j=1}^{N}|\lambda_j|^L\right)\mathbb{E}_{\boldsymbol{\epsilon}}\left|\sup_{G\in\mathcal{G}^{(T)}}\sum_{n=1}^{N}\epsilon_n G_n\right|\right.$$

$$\left. + \left(\sum_{k=1}^{L-1} B^{(T)k}K\gamma^k \sum_{j=1}^{N}|\lambda_j|^k + \gamma^L B^{(T)L}\sum_{j=1}^{N}|\lambda_j|^L\right)D\right] \tag{19}$$

$$+ (1-\mu)2^{5/2}\frac{B^{(T+1)}B^{(A)}\sqrt{MU}}{(M+U)}\sum_{i=1}^{N}|\lambda_i|$$

Considering the node feature based layers in (19), we can apply simplification as

$$\bar{\mathcal{R}}(\tilde{\mathcal{G}}^{(T)}, p) \leq 2\bar{\mathcal{R}}(\mathcal{G}^{(T)}, p)$$

$$= 2\mathbb{E}_{\boldsymbol{\epsilon}}\left[\sup_{G_{\cdot c}\in\mathcal{G}^{(T-1)}, w\in\mathbb{R}^{C_T}:\|w\|_1\leq B^{(T)}}\left|\sum_{n=1}^{N}\epsilon_n\sum_{c=1}^{C_T}G_{nc}w_c\right|\right]$$

$$= 2\mathbb{E}_{\boldsymbol{\epsilon}}\left[\sup_{Z_{\cdot c}\in\mathcal{G}^{(T-1)}, w\in\mathbb{R}^{C_T}:\|w\|_1\leq B^{(T)}}\left|\sum_{c=1}^{C_T}\sum_{n=1}^{N}\epsilon_n G_{nc}w_c\right|\right]$$

$$= 2B^{(T)}\mathbb{E}_{\boldsymbol{\epsilon}}\left[\sup_{G_{n\cdot}\in\mathcal{G}^{(T-1)}}\left|\sum_{n=1}^{N}\epsilon_n G_{n\cdot}\right|\right],$$

which by repeating on all hypothesis classes $\mathcal{G}^{(l)}$, $l = T-1, \ldots, 1$, we obtain

$$\bar{\mathcal{R}}(\tilde{\mathcal{G}}^{(1)}, p) = 2^{T-1}\prod_{l=1}^{T-1}B^{(l)}\mathbb{E}_{\boldsymbol{\epsilon}}\left[\sup_{G_{n\cdot}\in\mathcal{G}^{(0)}}\left|\sum_{n=1}^{N}\epsilon_n G_{n\cdot}\right|\right]. \tag{20}$$

Now, we bound

$$\bar{\mathcal{R}}(\tilde{\mathcal{G}}^{(0)}, p) \leq 2\bar{\mathcal{R}}(\mathcal{G}^{(0)}, p)$$

$$= 2\mathbb{E}_{\boldsymbol{\epsilon}}\left[\sup_{w\in\mathbb{R}^{C_0}:\|w\|_1\leq B^{(0)}}\left|\sum_{n=1}^{N}\sum_{c=1}^{C_0}\epsilon_n X_{nc}w_c\right|\right]$$

$$= 2B^{(0)}\mathbb{E}_{\boldsymbol{\epsilon}}\left[\max_{c\in[C_0]}\left|\sum_{n=1}^{N}\epsilon_n X_{nc}\right|\right]$$

$$\leq 2B^{(0)}\mathbb{E}_{\boldsymbol{\epsilon}}\left[\left\|\sum_{n=1}^{N}\epsilon_n X_{n\cdot}\right\|_2\right]$$

$$\leq 2B^{(0)}\sqrt{\mathbb{E}_{\boldsymbol{\epsilon}}\sum_{c=1}^{C_0}\left(\sum_{n=1}^{N}\epsilon_n X_{nc}\right)^2} \quad \text{(Jensen Inequality)}$$

$$= 2B^{(0)}\sqrt{\mathbb{E}_{\boldsymbol{\epsilon}}\sum_{c=1}^{C_0}\sum_{n,m=1}^{N}\epsilon_n\epsilon_m X_{nc}X_{mc}}$$

$$= 2B^{(0)}\sqrt{\sum_{c=1}^{C_0}\sum_{m=1}^{N}2p(X_{mc})^2}$$

$$= 2B^{(0)}\sqrt{2p}\|X\|_{\mathrm{F}}.$$

Furthermore, given that $p = p_0 = \frac{MU}{(M+U)^2}$, we have

$$\bar{\mathcal{R}}(\tilde{\mathcal{G}}^{(0)}, p_0) \leq 2B^{(0)}\sqrt{\frac{2MU}{(M+U)^2}}\|X\|_{\mathrm{F}}. \tag{21}$$

14

Method	Cora	Citeseer	Pubmed
Classes	7	4	3
Nodes	2708	3327	19717
Edges	5429	4732	44338
Features	1433	3703	500
Edge Homophily	0.825	0.718	0.792
MLP	74.46±2.08	73.41±1.82	87.60±0.31
GCN	87.22±1.09	76.26±1.49	88.11±0.45
SGC	87.22±1.06	76.37±1.49	88.01±0.49
GCNII	**88.16±1.20**	**76.95±1.48**	89.48±0.59
GPRGNN	**87.76±1.25**	**76.80±1.59**	89.43±0.57
APPNP	**88.00±1.16**	**77.19±1.86**	89.38±0.38
LINK	80.88±1.35	65.41±3.49	81.16±0.32
LINKX	84.64±1.13	73.19±0.99	87.86±0.77
GPCN	86.29±1.33	76.16±1.76	**89.72±0.49**
GPCN-LINK	86.03±0.85	75.45±1.64	**89.85±0.33**
AGPCN	86.23±1.65	74.86±1.52	**89.48±0.50**
AGPCN-LINK	85.25±2.73	74.08±3.71	89.21±0.45

Table 4: Properties and node-classification accuracy of homophilic datasets. The best three results are highlighted.

and combining (20) and (21) with (19), we arrive at the final bound

$$Q^{-1}\bar{\mathcal{R}}(\tilde{\mathcal{F}}_{\mu,\gamma}, p_0) \le C' B^{(T+1)} \mu \bigg[2^T \prod_{l=0}^{T-1} B^{(l)} \sqrt{\frac{2MU}{(M+U)^2}} \bigg(I + \sum_{k=1}^{L-1} B^{(T)k} L\gamma^k \sum_{j=1}^{N} |\lambda_j|^k$$

$$+ \gamma^K B^{(T)L} \sum_{j=1}^{N} |\lambda_j|^L \bigg) \|X\|_{\mathrm{F}} + \bigg(\sum_{k=1}^{L-1} B^{(T)k} L\gamma^k \sum_{j=1}^{N} |\lambda_j|^k$$

$$+ \gamma^K B^{(T)L} \sum_{j=1}^{N} |\lambda_j|^L \bigg) D \bigg] + (1-\mu) 2^{5/2} \frac{B^{(T+1)} B^{(A)} \sqrt{MU}}{(M+U)} \sum_{i=1}^{N} |\lambda_i|.$$

Proof of Theorem 2. We modify the following hypothesis class (10) to suit AGPCN-LINK as

$$\mathcal{F}_{\mu,\gamma} = \bigg\{ X, \bar{A} \mapsto \text{softmax}\bigg(f^{(3)} \circ (\mu f^{(1)} \circ g^{(T)} \circ \cdots \circ g^{(0)}(X) + (1-\mu) f^{(2)}(\bar{A})) |$$

$$g^{(l)}(Z) = \text{Relu}(ZW^{(l)}), f^{(1)}(X_T) = \theta_0 X_T + \sum_{k=1}^{L} \theta_k \bar{A}^k X_T W^{(T)k} \bigg),$$

$$f^{(2)}(\bar{A})) = \bar{A} W^{(A)}, \ f^{(3)}(Z) = ZW^{(T+1)}, \ \|W_{\cdot c}^{(l)}\|_1 \le B^{(l)} \text{ for all } c \in [C_{l+1}], \|W_{\cdot c}^{(A)}\|_1 \le B^{(A)} \bigg\}.$$

Following a similar proof procedure as in Theorem 1 we arrive at the bound the desired bound.

C   Experiments with Homophilous Data

Table 4 shows performances for homophilous graphs Cora, Citeseer, and Pubmed from Pei et al. (2020). Both GPCN and GPCN-LINK have obtained with low accuracy for Cora and Citeseer while GCNII, GPRGNN, and APPNP have given the best accuracy. Further, note that LINKX only gives a weak accuracy for these datasets. For the Pubmed dataset, GPCN and GPCN-LINK have given the best accuracy outperforming previous best results from GCNII, GPRGNN, and APPNP. Overall, GPCN and its varaints have shown the ability obtain better accuracy compared to LINK and LINKX while giving competitive performances with respect to other graph convolution models.

D   Ablation Studies

We carried out ablation studies to understand the robustness of proposed models against oversmoothing due to polynomial structure of scaling parameters and weights. For ablation experiments, we select the best hyperparameter
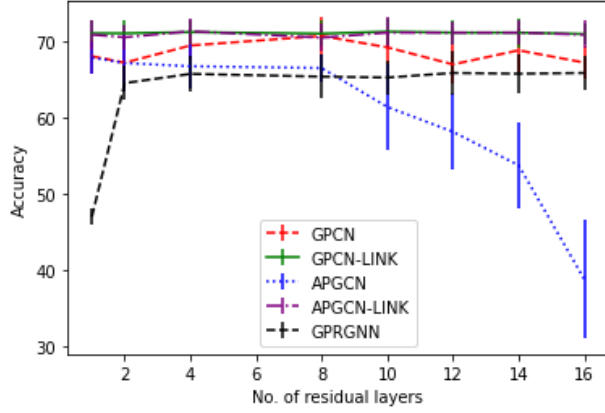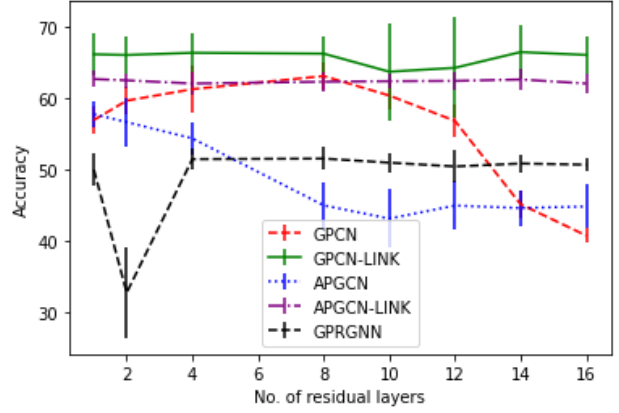
Figure 1: Ablation study on Chameleon

Figure 2: Ablation study on Squirrel

Dataset	Learning rate	Hidden	Weight decay	T	MLP	γ	Dropout
Cora	0.05	64	0.001	2	1	1	0.6
Citeseer	0.01	64	0.001	2	1	0.25	0.3
Pubmed	0.01	64	0.001	4	2	0.0625	0.3
Chameleon	0.01	512	0.001	8	1	0.25	0.3
Squirrel	0.05	512	1e-5	8	1	0.0625	0.3
Actor	0.05	512	0.01	2	2	0.0625	0.0
Cornell	0.01	512	0.001	2	4		0.3
Texas	0.01	512	0.001	1	3	0.015625	0.6
Wisconsin	0.05	512	0.001	2	1	0.0625	0.3
Twitch-DE	0.01	512	0.001	2	1	16	0.0
Penn94	0.05	512	1e-5	4	1	0.0625	0.0
Yelp-Chi	0.01	64	1e-5	4	4	0.0625	0.0
Deezer-Europe	0.01	64	1e-5	16	5	0.0625	0.0
Genius	0.01	64	1e-5	8	1	0.0625	0.0

Table 5: Hyperparameters for GPCN

selection for a dataset and change the scaling parameter (γ) in the range of $2^0, 2^{-2}, \ldots, 2^{-8}$, residual layers $L = 1, 2, 4 \ldots, 16$, and dropout $\in (0.0, 0.3, 0.6, 0.9)$ while keeping the rest of the parameters (learning rate, hidden,...etc) fixed.

Figure 1 shows that node calssification accuracy for Chameleon with GPCN-LINK and APGCN-LINK do not decrease in accuracy as the number layers increases, hence, rubust against oversmoothing. GPCN is relatively stable with increasing layers though the accuracy is low compared to GPCN-LINK and APGCN-LINK. APGCN shows strong oversmoothing, however, gives a higher accuracy compared to GPRGNN with one residual layer. Similar behaviours are seen with Squirrel (Figure 2) where GPCN and AGPCN show oversmoothing and other models are robust against oversmoothing.

A common feature among all the proposed methods is that they provide higher accuracy at low number of residual layers. This observation is with agreement with the theoretical analysis in Section 4.

E   Hyperparameter Summary

In this section, we provide hyperparameters selected for out proposed methods. Hyperparameters are selected for all models (where applicable) from hidden $\in \{64, 512\}$, learning parameter $\in \{0.01, 0.05\}$ for the Adam method, weight decay $\in \{0.0, 0.001, 0.00001\}$, initial feature learning layers $T \in \{1, 2, 3, 4, 5\}$, residual layers $L \in \{1, 2, 4, 8\}$, $\gamma \in \{2^8, 2^6, \ldots, 2^0, 2^{-2}, \ldots, 2^6\}$, dropout $\in \{0, 0.3, 0.6, 0.9\}$.

Dataset	Learning rate	Hidden	Weight decay	T	MLP	γ	Dropout
Cora	0.01	512	0.001	2	1	4	0.6
Citeseer	0.001	64	1e-5	1	1	64	0.3
Pubmed	0.01	512	0.001	4	3	0.0625	0.3
Chameleon	0.01	512	0.001	4	2	0.00390625	0.6
Squirrel	0.05	512	1e-5	8	1	4	0
Actor	0.01	64	0.001	4	3	0.0625	0.0
Cornell	0.01	512	0.001	1	4	0.015625	0
Texas	0.01	512	0.001	1	4	0.00390625	0
Wisconsin	0.01	512	0.001	2	3	0.25	0
Twitch-DE	0.01	64	0.001	2	2	64	0.0
Penn94	0.01	512	1e-5	4	1	4	0.0
Yelp-Chi	0.01	512	1e-5	2	5	0.015625	0.0
Deezer-Europe	0.01	512	0.001	1	8	3	0.0
Genius	0.01	64	0.001	8	2	1	0.0

Table 6: Hyperparameters for GPCN-LINK

Dataset	Learning rate	Hidden	Weight decay	T	MLP	Dropout
Cora	0.05	512	0.001	2	1	0.6
Citeseer	0.01	512	0.001	2	1	0.6
Pubmed	0.01	64	0.0	2	2	0.3
Chameleon	0.01	512	0.001	1	1	0.6
Squirrel	0.01	64	0.001	1	1	0.3
Actor	0.05	64	0.001	2	1	0.3
cornell	0.05	512	0.001	1	2	0.3
Texas	0.05	512	0.001	1	2	0.3
Wisconsin	0.05	512	0.001	1	2	0.3
Twitch-DE	0.01	512	1e-5	2	1	0.0
Penn94	0.01	64	1e-5	8	2	0.3
Yelp-Chi	0.01	512	1e-05	2	2	0.0
Deezer-Europe	0.01	64	1e-5	1	2	0.6
Genius	0.01	512	1e-5	2	2	0.0

Table 7: Hyperparameters for AGPCN

Dataset	Learning rate	Hidden	Weight decay	T	MLP	Dropout
Cora	0.01	512	0.001	2	1	0.6
Citeseer	0.01	512	0.001	2	1	0.6
Pubmed	0.01	512	0.001	2	2	0.3
Chameleon	0.05	64	0.001	2	1	0.3
Squirrel	0.05	512	1e-5	8	1	0.3
Actor	0.01	512	0.001	8	2	0.0
cornell	0.01	64	0	4	3	0.0
Texas	0.01	512	0.001	1	4	0.3
Wisconsin	0.01	512	0.001	2	2	0.0
Twitch-DE	0.01	64	0.001	4	2	0
Penn94	0.01	64	1e-5	4	2	0.3
Yelp-Chi	0.01	512	1e-5	2	3	0.0
Deezer-Europe	0.01	512	1e-5	1	2	0.6
Genius	0.01	64	1e-5	4	2	0.3

Table 8: Hyperparameters for AGPCN-LINK